J Fluoresc (2015) 25:473–479
DOI 10.1007/s10895-015-1547-8

ORIGINAL PAPER

Novel Pyridinium Inner Salt Dye and its Complexes: Synthesis, Crystal Structures and Photophysical Properties

Yong-Hong Zhou · Na-Li Wang · Ti-Fang Miao · Juan-Gang Wang · Zhe-Yu Wang

Received: 12 December 2014 / Accepted: 23 February 2015 / Published online: 3 March 2015

Abstract Two novel metal complexes, namely $[Tb_2(L)_6(H_2O)_4]\cdot(NO_3)_6\cdot L_2\cdot(H_2O)_{18}$ (**1**) and $[Hg(L)Cl_2]_n$ (**2**), were obtained by the reaction of D-π-A (D=donor, π=conjugated spacer, A=acceptor) type pyridinium inner salt dye, *trans*-4-[(*p*-*N*,*N*-dimethylamino)styryl]-*N*-(2-propanoic-acid) pyridinium (**L**) with corresponding metal salts. Single crystal *X*-ray diffraction analyses reveal that compound **1** possesses dinuclear motif in which two Tb(III) ions are linked by four carboxylate groups while complex **2** exhibits 1D chain structure based on Hg(II) ions bridged by carboxylate groups. The linear and non-linear optical properties of complexes **1** and **2** have been studied. Both **1** and **2** exhibit intense single-photon excited fluorescence (SPEF) and two-photon excited fluorescence (TPEF) in the red range. Results show that the replacement of central ions from Hg^{2+} to Tb^{3+} influence the two-photon absorption cross-section significantly through increasing the density of the chromophore. However, the peak positions of two-photon excited fluorescence are only slightly affected. Compared with **L** molecule, complex **1** shows enhanced two-photon absorption cross-section and decreased fluorescent lifetime.

Keywords Two-photon absorption · Metal complex · Pyridinium inner salt dye · Two-photon excited fluorescence

Y.-H. Zhou (✉) · N.-L. Wang · T.-F. Miao · J.-G. Wang
School of Chemistry and Material Science, Huaibei Normal University, Huaibei 235000, People's Republic of China
e-mail: zhou21921@sina.com

Z.-Y. Wang
No. 1 High School of Huaibei, Huaibei 235000, People's Republic of China

Introduction

Recent years have witnessed the rapidly growing interest on the design and synthesis of materials with two-photon absorption (TPA) activity. The motivation arises from their promising applications in biosensing technology [1], optical data storage [2,3], optical power limiting [4], two-photon laser scanning microscopy [5], and up-conversion lasing [6]. In order to realize these applications, materials with large two-photon absorption cross-sections (σ) are demanded [7]. Research in this field has been focused on the design and fabrication of new efficient two-photon absorbers, and the exploration of the relationship between the structures and properties. To date, several effective design approaches have been applied to enhance the σ value [8–10], and it has been revealed that the length of π-conjugated spacer, strength of donor/acceptor motifs and the molecular planarity, play important roles in tuning the molecular TPA activity of materials [11–13]. In particular, it has been found that TPA effect enhances with the increase of chromophore number density. Therefore, efficient two-photon absorbers, such as quadrupolar, octupoles and multi-branched chromophores have been extensively developed [14–19]. However, although metal ions can serve as multi-dimensional templates, able to assemble ligands into multi-branched molecules by providing enough coordination sites, it is only recently that metal complexes as potential TPA materials have been investigated [20]. Prasad et al. demonstrated the enhancement of TPA cross-section upon coordination to Ni(II) of phenanthrolines with weaker electron-donating group, while a decrease of the TPA effect was found when Ni(II) ions were coordinated to phenanthrolines possessing strong electron donors [20]. Bharadwaj and co-workers observed that a Schiff base exhibits exceptionally high σ values upon binding with Zn(II) or Cu(I) ions, underlining the importance of the metal ion [21]. Recently, we reported a series of rare earth complexes with

Table 1 Crystal data for compounds 1, 2 and L·5H_2O

Compound	L·5H_2O	1	2
Formula	$C_{18}H_{30}N_2O_7$	$C_{144}H_{204}N_{22}O_{56}Tb_2$	$C_{18}H_{20}Cl_2HgN_2O_2$
Formula weight	386.44	3457.14	567.85
Crystal system	Triclinic	Monoclinic	Monoclinic
Space group	P-1	$P2_1/n$	$P2_1/m$
Unit cell dimensions			
a(Å)	7.1217(6)	21.9340(18)	5.0460(4)
b(Å)	12.4646(11)	16.9957(14)	12.1629(11)
c(Å)	12.5366(12)	22.083(2)	16.1941(14)
α(°)	106.847(2)	90	90
β(°)	92.2300	102.574(2)	96.3670
γ(°)	104.440(2)	90	90

intense TPA and frequency up-conversion emission. In these complexes, two D-π-A type chromophores with large two-photon absorption cross section, *trans*-4-[(*p*-*N*,*N*-dimethylamino)styryl]-*N*-acetic-acid pyridinium and *trans*-4-[(*p*-*N*-2-hydroxyethyl-*N*-methylamino)styryl]-*N*-acetic-acid pyridinium, were used as ligands. Rare earth ions play an important role in determining the TPA properties of the complexes by adjusting the density of the chromophores [6]. These studies have highlighted the important roles of both the central ions and the chromophores to enhance the TPA responses of such materials.

To better understand the relationship between the density of chromophore and TPA activity, and to explore new materials with large TPA cross section, we present here one novel stilbene-pyridinium salt dye, *trans*-4-[(*p*-*N*,*N*-dimethylamino)styryl] -*N*-(2-propanoic-acid) pyridinium (**L**), and a dinuclear complex $[Tb_2(L)_6(H_2O)_4]\cdot(NO_3)_6\cdot L_2\cdot(H_2O)_{18}$ (**1**) with high density of **L** (chromophore). In order to investigate the role of metal ions in determining the TPA effect, another metal complex, $[Hg(L)Cl_2]_n$ (**2**), is also reported. All three compounds have been fully characterized. The linear absorption, single-photon excited fluorescence (SPEF) and two-photon excited fluorescence (TPEF) spectra of these compounds were systematically investigated.

Table 2 Selected bond lengths (Å) and bond angles (°) for compounds L 5H_2O and 1–2

L·5H_2O			
C(1)-O(1)	1.253(3)	C(1)-O(2)	1.233(3)
C(2)-N(1)	1.489(3)	C(6)-C(9)	1.459(4)
C(9)-C(10)	1.309(4)	C(10)-C(11)	1.460(4)
O(1)-C(1)-O(2)	126.6(3)	N(1)-C(2)-C(1)	110.0(2)
Complex 1			
Tb(1)-O(2A)	2.299(7)	Tb(1)-O(3)	2.310(9)
Tb(1)-O(4A)	2.330(9)	Tb(1)-O(9)	2.335(8)
Tb(1)-O(10)	2.377(10)	Tb(1)-O(1)	2.402(8)
Tb(1)-O(5)	2.428(8)	Tb(1)-O(6)	2.540(10)
Complex 2			
Hg(1)-Cl(1)	2.311(7)	Hg(1)-Cl(1A)	2.311(7)
Hg(1)-O(2B)	2.41(3)	Hg(1)-O(1)	2.57(2)

Experimental

Materials and Instruments

All chemicals used in the synthesis are of analytical grade and used without further purification. Elemental analyses for C, H and N were carried out on a Vario EL IIIanalyzer. Infrared spectra were recorded using KBr pellets with a Nicolet 510 FT-IR spectrometer in the range of 4000–400 cm^{-1}. UV–vis absorption spectra were performed on a Shimadzu UV3600 UV–vis-NIR spectrophotometer. Single-photon excited fluorescence spectra were measured with a RF-5301PC spectrophotometer at room temperature.

Synthesis

*Synthesis of Trans-4-[(p-N,N-dimethylamino)styryl] -N-(2-propanoic-acid) Pyridinium (**L**)*

L·5H_2O was synthesized using the literature method [6] except that 2-bromopropionic acid was used instead. Yield: 25 %. Anal. Calc. for $C_{18}H_{30}N_2O_7$: C 55.89, H 7.76, N 7.24 %. Found: C 55.91, H 7.75, N 7.27 %. IR (cm^{-1}): 3411 s; 1635vs; 1592vs; 1388vs; 1187vs; 807w; 535w.

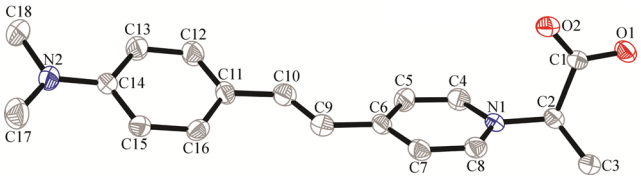

Fig. 1 Molecular structure of compound L

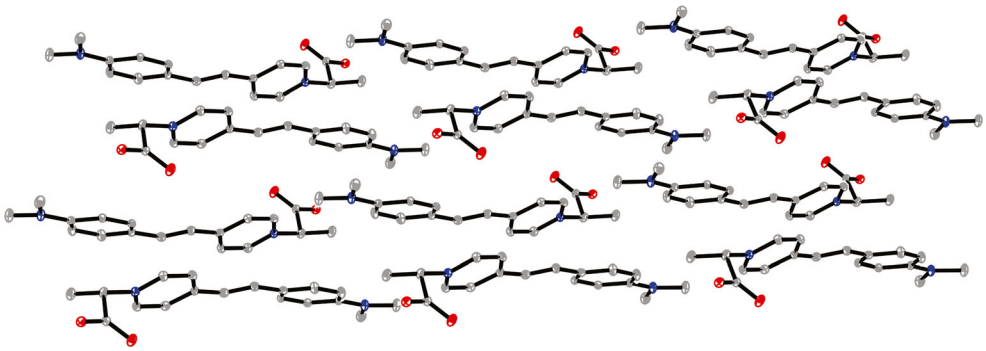

Fig. 2 Packing diagram for compound L

*Synthesis of $[Tb_2(L)_6(H_2O)_4]\cdot(NO_3)_6\cdot L_2\cdot(H_2O)_{18}$ (**1**)*

$Tb(NO_3)_3\cdot 6H_2O$ (0.136 g, 0.3 mmol) and **L** (0.296 g, 1 mmol) were dissolved in 20 mL ethanol and refluxed at 70 °C for 8 h, then naturally cooled to room temperature. Dark red crystals suitable for *X*-ray diffraction of **1** were obtained by slow evaporation of the mother liquid. Yield: 55 %. Anal. Calc. for $C_{144}H_{204}N_{22}O_{56}Tb_2$: C 49.98, H 5.90, N 8.91 %. Found: C 50.01, H 5.86, N 8.93 %. IR (cm^{-1}): 3391vs; 1645vs; 1587vs; 1381vs; 1177vs; 821w; 536w.

*Synthesis of $[Hg(L)Cl_2]_n$ (**2**)*

The mixture of $HgCl_2$ (0.136 g, 0.5 mmol) and **L** (0.296 g, 1 mmol) was dissolved in 20 mL ethanol and refluxed at 70 °C for 5 h, and then cooled to room temperature slowly. Dark red crystals of **2** were isolated by slow evaporation of the mother liquid. Yield: 75 %. Anal. Calc. for $C_{18}H_{20}N_2O_2Cl_2Hg$: C 38.04, H 3.52, N 4.93 %. Found: C 38.01, H 3.56, N 4.95 %. IR (cm^{-1}): 1642vs; 1587vs; 1381vs; 1182vs; 812w; 539w.

Structure Determination

Single crystal *X*-ray diffraction data of **L**, **1** and **2** were collected on a Bruker SMART APEX CCD diffractometer with graphite monochromated Mo Kα radiation (λ=0.71073 Å) at 298 K using ω-scan technique. The structures were solved by direct method and refined using the SHELXL-97 program [22]. All of the non-hydrogen atoms were refined with anisotropic temperature factors and hydrogen atoms were added geometrically. Crystallographic data for three compounds are summarized in Table 1, selected bond lengths and angles are listed in Table 2.

Results and Discussion

Structural Features

As depicted in Fig. 1 for compound **L**, the total angles around N2 (C18-N2-C17, 116.8(3)°; C18-N2-C14, 121.3(3)°; C14-N2-C17, 121.1(3)°) are close to 360° (359.4°), therefore the trigonal NC_3 is perfectly coplanar. Actually, the whole aniline section is almost coplanar. This conformation of the N-based donor set suggests that the lone pair of electrons can be easily delocalized into the π-center. The least-square plane calculations indicate that the pyridinium and benzene rings are twisted by 22.9°. The C-C bond distances of benzene and pyridinium rings fall into the range of C-C single bond (1.54 Å) and C=C double bond (1.34 Å). The spacers between the benzene and pyridinium rings are highly conjugated with bond lengths of C6-C9 and C10-C11 are 1.459(4) Å and 1.460(4) Å, respectively. These structural characters suggest that **L** possesses highly π-conjugated systems, leading to the charge transfer from donor to acceptor, making **L** molecule a promising candidate for TPA materials [23].

Prasad et al. have proposed that the inner salt molecule prefers to interact with adjacent ones in head-to-tail, side-by-side or chain-like fashions to reach a favorable configuration. As shown in Fig. 2, **L** molecules are stacked in chain-like oligomer configuration, confirming the hypothesis of Prasad.

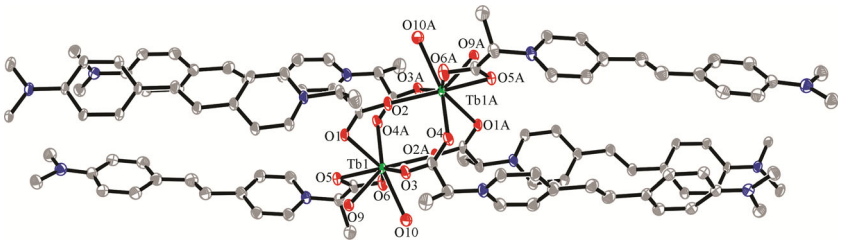

Fig. 3 The coordination environment for Tb(III) centres in complex 1

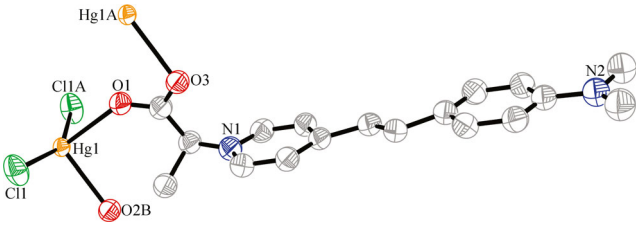

Fig. 4 The coordination environment for Hg(II) centres in 2

This packing fashion results in conformational rigidity and provides an entropically favorable state of the inner salt molecules, which would enhance the TPA effect [24].

Compound **1** consists of two Tb(III) ions, six coordinated **L** ligands and four coordinated H_2O, six NO_3^- anions, two uncoordinated **L** molecules and eighteen lattice H_2O. As shown in Fig. 3, the Tb(III) is eight-coordinated by six oxygen atoms from five independent **L** ligands, the other coordinated sites are completed by two oxygen atoms from two water molecules. The Tb-O distances are close to those of corresponding Tb(III) complexes [25]. Eight **L** molecules in **1** can be divided into three types: four **L** molecules with their carboxyl groups acting as bridges, link two Tb(II) atoms to form a novel $[Tb_2L_4]$ unit with Tb ···Tb separation of 4.195 Å, which is comparable with that in analogous complex [26]; another two **L** ligands are chelated to the Tb(III) atom, while the other two **L** molecules crystallize as lattice molecules.

Complex **2** adopts one-dimensional (1D) chain structure. As shown in Fig. 4, each Hg(II) atom lies in a distorted tetrahedron coordination geometry, which is completed by two Cl^- anions and two carboxyl oxygen atoms from two **L** ligands. The bond angles around Hg(II) atom are in the range of 89.1(8)-151.4(4)° and Hg-Cl, Hg-O bond lengths are 2.311(7) Å and 2.41(3) Å, respectively. The Hg-O distance found here is significantly shorter than that observed in Cu(2-pyrazinecarboxylate)$_2$HgCl$_2$ (2.736(4) Å) [27], while the Hg-Cl distance is comparable to those found in related Hg(II) complexes [27]. The carboxyl group of **L** ligand possesses bidentate bridging coordination mode, linking symmetry-related Hg(II) atoms, giving rise to the formation of a 1D $[Hg(COO)_2]$ chain along *b* axis. The **L** ligands are parallel attached to the chain, as shown in Fig. 5.

Table 3 Linear and non-linear optical properties of **L** and complexes **1-2**

compound	λ_{max} (abs)/ nm	λ_{max} (SPEF)/ nm	λ_{max} (TPEF)/ nm	σ/ GM[a]	lifetime/ ps
L	457	579	613	69.5	112
1	460	582	622	211.6	65
2	460	579	615	65.8	86

[a] The TPA cross section: $1GM=10^{-50}$ cm^4 s $photon^{-1}$

It should be pointed out that after coordinated to the metal ions, the bond lengths, angles and the planarity of **L** are almost identical to that of the free **L** ligands, which indicates that metal ions have few influence on the electron distribution in the ligands. In addition, Tb^{3+} ions possess higher coordination number than Hg^{2+} ion. As a result, Tb^{3+} ion can be assembled with more chromophores; in fact, there are eight **L** ligands in **1**, whereas only one **L** ligand exists in **2**. The increased density of chromophore is important for the enhancement of TPA cross section.

Linear Absorption and Single-Photon Excited Fluorescence

Linear absorption spectra of complexes **1**, **2** and **L** were performed on a Shimadzu UV3600 UV–vis-NIR spectrophotometer using dilute solutions (10^{-5} mol/L in DMF). Their absorption maxima are 457, 460 and 460 nm, for **L**, **1** and **2**, respectively (Table 3). A representative linear absorption spectrum of complex **1** is depicted in Fig. 6. The similarity of the absorption indicates that the linear absorption can be attributed to the **L** ligands, and the metal ions almost have no influence on the energy gap between the ground state and the first

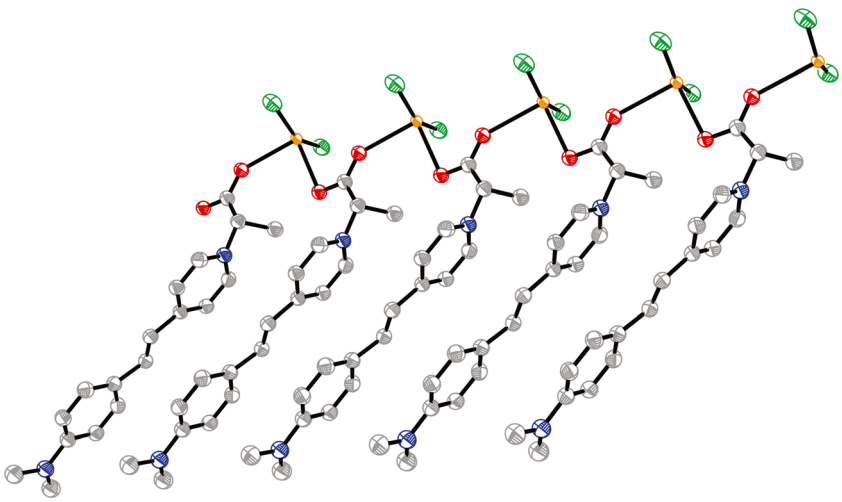

Fig. 5 The 1D chain formed by L ligands and Hg(II) ions in 2

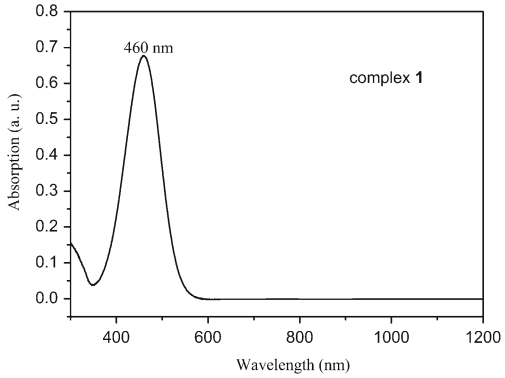

Fig. 6 Linear absorption spectrum of complex 1 in DMF

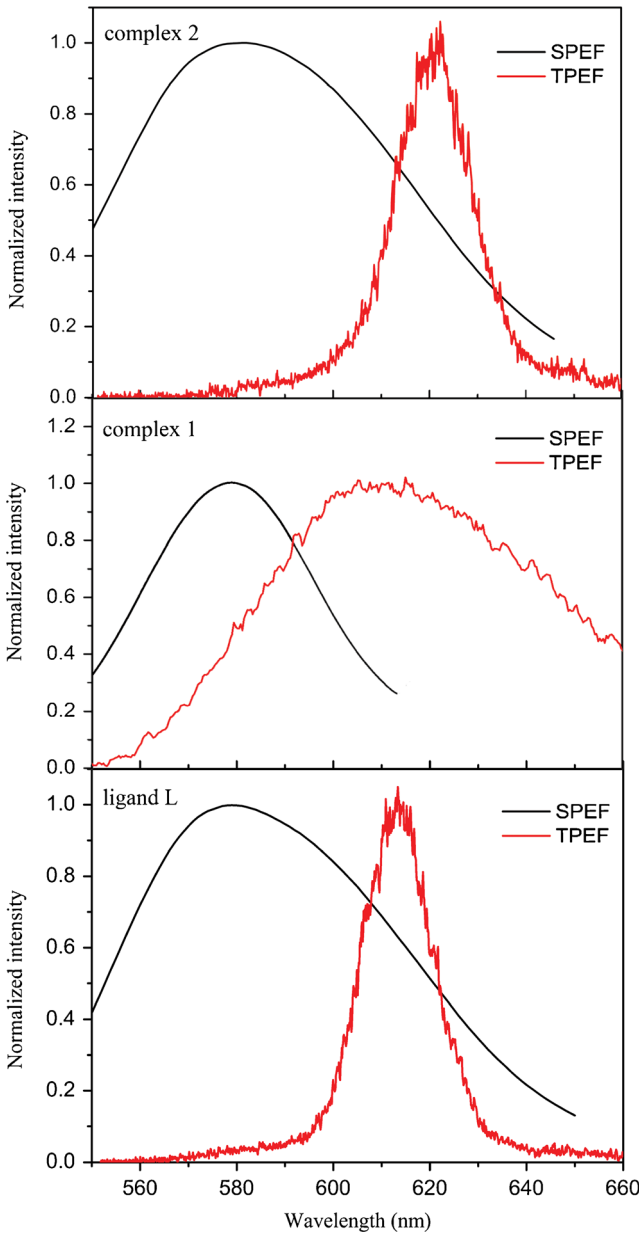

Fig. 7 Single- and two-photon excited fluorescence spectra of compounds 1, 2 and L in DMF

excited state of **L** molecule, which are associated with their structural characters as discussed above [6]. The absorbance values follow the order: **1**>**2**≈**L**, the increased density of chromophore in **1** (density of the chromophore is 8 per molecule) may be responsible for the largest absorbance value compared to those of **2** and **L**. Notably, no absorption in the spectral range from 600 to 1200 nm was observed. Then, any emission at this region can be assigned to a simultaneous two-photon absorption process.

Figure 7 gives the single-photon excited fluorescence spectra (SPEF) of 10^{-6} mol/L solution of compounds **1**, **2** and **L** in DMF. We can see that SPEF peaks are located at 582 nm for **1**, 579 nm for **2** and 579 nm for **L**, respectively.

Two-photon Absorption Properties

Two-photon excited fluorescence (TPEF) of the as-synthesized compounds were measured in 10^{-3} mol/L DMF solution with a 1064 nm laser beam as excited source, and a streak camera (Hamamatsu model 5680) as a recorder. The picosecond Nd:

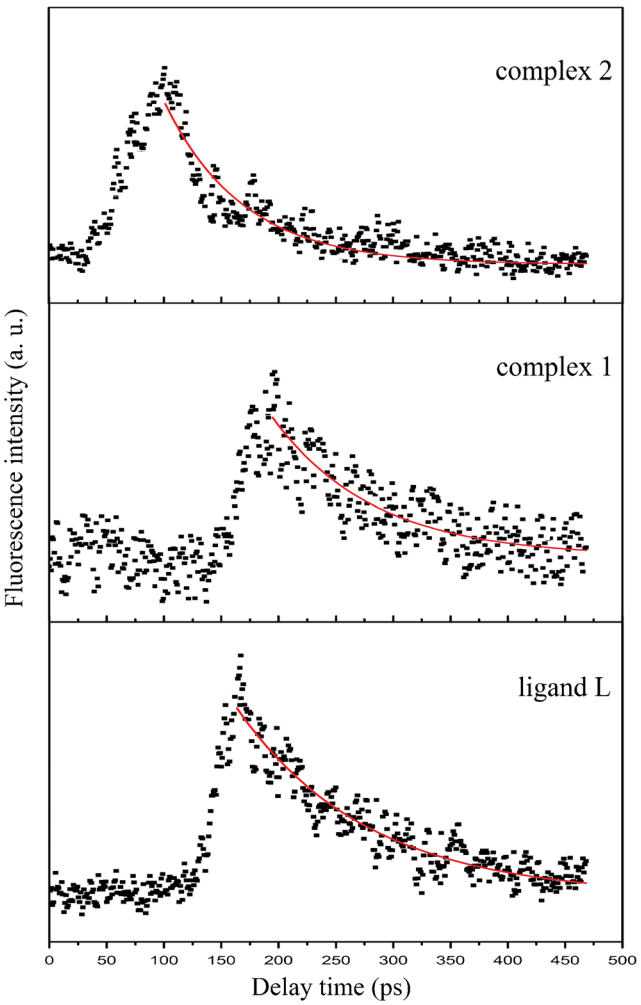

Fig. 8 Two-photon-excited fluorescence lifetimes of 0.01 mol/L compounds 1, 2 and L in DMF

YAG laser has a pulse duration of 40 ps with repletion rate of 10 Hz. As shown in Fig. 7 and Table 3, **L** exhibits intense TPEF emission at 613 nm, which is close to that of complex **2**, while that for complex **1** is red-shifted about 9 nm. The peak positions of TPEF spectra are red-shifted 34–40 nm compared to those of the corresponding SPEF spectra. This phenomenon can be explained by the so-called "reabsorption effect". Comparing Fig. 6 with Fig. 7, it can be found that there is an overlap between the red side of the absorption spectra and blue side of the fluorescence spectra. This overlap enlarges with the increase of the concentration. As for the single-photon excited fluorescence, dilute solutions were used and the reabsorption effect could be neglected, while the TPEF experiments were performed with concentrated solution, causing remarkable reabsorption.

The TPA cross-sections of complexes **1**, **2** and **L** were measured by open aperture Z-scan experiments with a fs-laser and the samples were dissolved in DMF. From Table 3, we can find that complex **1** shows a larger TPA cross-section value (211.6 GM) compared with **L** (69.5 GM). The enhanced TPA cross-section may arise from the high density of chromophore in complex **1**. The results further highlight the principle that increasing the chromophore density would lead to an enhancement of the TPA activity [28]. Additionally, the TPA cross-section value of complex **1** is 3.0 times that of **L**, not increasing proportionally to the chromophore density, which suggests that no strong cooperative enhancements occur between chromophores in such environment. In this respect, complex **1** can be regarded as a new type of non-conjugated dendrimer with Tb(III) as cores, being different from the conjugated dendrimers with pyridine-, imidazole- or phenylamine-cores [28–32]. On the other hand, complex **1** shows much larger TPA cross section than complex **2**, indicating that the TPA cross section of complexes can be easily tuned by varying the central metal ions for specific applications.

Figure 8 shows the fluorescence delay curves of **1**, **2** and **L** in DMF with concentration of 0.01 mol/L. The lifetimes are 65, 86, and 112 ps for **1**, **2** and **L**, respectively. The relatively long two-photon fluorescent lifetime of **L** can be explained by the TICT (twisted intramolecular charge transfer) model. When the molecules are induced to the excited state, the charge is transferred from the donor moiety through the π-bridge to the acceptor moiety, leading to the enhancement of charge density on the acceptor group. As discussed above, **L** molecules are self-assembled in a head-to-tail fashion, which offers an energy favorable manner and rigid structure. Therefore, the gap between the ICT and TICT might be enlarged, which in turn stabilizes the excited state of **L** molecules and enlarge the fluorescent lifetime [33]. Upon coordinated to the metal ions, the head-to-tail fashion of **L** ligands disappear, resulting in the decrease of barrier between the ICT and TICT states. Thus, the fluorescent lifetimes of complexes **1** and **2** decrease rapidly.

Conclusions

This work has demonstrated a facile synthesis of two-photon absorption materials through conventional coordination of metal ions with chromophore. This approach offers a convenient procedure to synthesize two-photon absorbing materials with large cross section. The number density of chromophore can be adjusted by varying central metal ions, and the physical properties of materials can be finely modulated for specific application by using different chromophores. Modifications of the chromophores and metal ions to achieve large TPA cross section for these complexes and their potential application for two-photon-pumped lasing are currently underway.

Acknowledgments This work was financially supported by Scientific Research Foundation of Anhui Provincial Education Department (KJ2014A228).

References

1. Jiang YH, Wang YC, Hua JL, Tang J, Li B, Qian SX, Tian H (2010) Multibranched triarylamine end-capped triazines with aggregation induced emission and large two-photon absorption cross-sections. Chem Commun 46:4689–4691
2. Zhang Z, Hu Y, Luo Y, Zhang Q, Huang W, Zou G (2009) Polarization storage by twophoton-induced anisotropy in bisazobenzene copolymer film. Opt Commun 282:3282–3285
3. Dvornikov AS, Walker EP, Rentzepis PM (2009) Two-photon three-dimensional optical storage memory. J Phys Chem A 113:13633–13644
4. Liu YQ, Wang H, Zhang J, Li SL, Wang CK, Ding HJ, Wu JY, Tian YP (2014) Synthesis, crystal structures and third-order nonlinear optical properties in the near-IR range of two novel Ni(II) complexes. Opt Mater 36:687–696
5. Tokar VP, Losytskyy MY, Ohulchanskyy TY, Kryvorotenko DV, Kovalska VB, Balanda AO, Dmytruk IM, Prokopets VM, Yarmoluk SM, Yashchuk VM (2010) Styryl dyes as two-photon excited fluorescent probes for DNA detection and two-photon laser scanning fluorescence microscopy of living cells. J Fluoresc 20:865–872
6. Tian YP, Li L, Zhou YH, Wang P, Zhou HP, Wu JY, Hu ZJ, Yang JX, Kong L, Xu GB, Tao XT, Jiang MH (2009) Design and synthesis of two new two-photon absorbing pyridine salts as ligands and their rare earth complexes. Cryst Growth Des 9:1499–1504
7. Tan YQ, Zhang Q, Yu JC, Zhao X, Tian YP, Cui YJ, Hao XP, Yang Y, Qian GD (2013) Solvent effect on two-photon absorption (TPA) of three novel dyes with large TPA cross-section and red emission. Dyes Pigments 97:58–64
8. Wang XM, Wang D, Zhou GY, Yu WT, Zhou YF, Fang Q, Jiang MH (2001) Symmetric and asymmetric charge transfer process of two-photon absorbing chromophores: bis-donor substituted stilbenes, and substituted styrylquinolinium and styrylpyridinium derivatives. J Mater Chem 11:1600–1605
9. He GS, Zheng QD, Yong KT, Erogbogbo F, Swihart MT, Prasad PN (2008) Two- and three-photon absorption and frequency upconverted emission of silicon quantum dots. Nano Lett 8:2688–2692
10. Zhang M, Li M, Zhao Q, Li F, Zhang D, Zhang J, Yi T, Huang C (2007) Novel Y-type two-photon active fluorophore: synthesis and application in fluorescent sensor for cysteine and homocysteine. Tetrahedron Lett 48:2329–2333

11. Bouit PA, Kamada K, Feneyrou P, Berginc G, Toupet L, Maury O, Andraud C (2009) Two photon absorption-related properties of functionalized bodipy dyes in the infrared range up to telecommunication wavelengths. Adv Mater 21:1151–1154
12. Terenziani F, Parthasarathy V, Pla-Quintana A, Maishal T, Caminade AM, Majoral JP, Blanchard-Desce M (2009) Cooperative two-photon absorption enhancement by through-space interactions in multichromophoric compounds. Angew Chem Int Ed 48:8691–8694
13. Wang H, Li Z, Shao P, Qin J, Huang ZL (2010) Two-photon absorption property of a conjugated polymer: influence of solvent and concentration on its property. J Phys Chem B 114:22–27
14. Belfield KD, Bondar MV, Yanez CO, Hernandez FE, Przhonska OV (2009) Two-photon absorption and lasing properties of new fluorene derivatives. J Mater Chem 19:7498–7502
15. Padilha LA, Webster S, Przhonska OV, Hu HH, Peceli D, Rosch JL, Bondar MV, Gerasov AO, Kovtun YP, Shandura MP, Kachkovski AD, Hagana DJ, Stryland EWV (2009) Nonlinear absorption in a series of donor-pi-acceptor cyanines with different conjugation lengths. J Mater Chem 19:7503–7513
16. Pucher N, Rosspeintner A, Satzinger V, Schmidt V, Gescheidt G, Stampfl J, Liska R (2009) Structure-activity relationship in D-pi-A-pi-D-based photoinitiators for the two-photon-induced photopolymerization process. Macromolecules 42:6519–6528
17. Albota M, Beljonne D, Brédas JL, Ehrlich JE, Fu JY, Heikal AA, Hess SE, Kogej T, Levin MD, Marder SR, McCord-Maughon D, Perry JW, Rockel H, Rumi M, Subramaniam G, Webb WW, Wu XL, Xu C (1998) Design of organic molecules with large two-photon absorption cross sections. Science 281:1653–1656
18. Li L, Wu Y, Zhou Q, He C (2012) Experimental and theoretical studies on the one-photon and two-photon properties of a series of carbazole derivatives containing styrene. J Phys Org Chem 25:362–372
19. Xiao HB, Mei C, Li B, Ding N, Zhang YZ, Wei TT (2013) Synthesis, solvatochromism and large two-photon absorption cross-sections of water-soluble dipicolinate-based pyridinium salts. Dyes Pigments 99: 1051–1055
20. Zheng Q, He GS, Prasad PN (2005) Novel two-photon-absorbing, 1, 10-phenanthroline-containing π-conjugated chromophores and their nickel(II) chelated complexes with quenched emissions. J Mater Chem 15:579–587
21. Das S, Nag A, De G, Bharadwaj PK (2006) Zinc(II)- and Copper(I)-mediated large two-photon absorption cross sections in a bis-cinnamaldiminato schiff base. J Am Chem Soc 128:402–403
22. SHELXTL (version 5.10) (1994) Siemens Analytical X-ray Instruments Inc.: Madison, WI
23. Ren Y, Fang Q, Yu WT, Lei H, Tian YP, Jiang MH, Yang QC, Mak TCW (2000) Synthesis, structures and two-photon pumped up-conversion lasing properties of two new organic salts. J Mater Chem 10:2025–2030
24. Zheng QD, He GS, Lin TC, Prasad PN (2003) Synthesis and properties of substituted (p-aminostyryl)-1-(3-sulfooxypropyl)pyridinium inner salts as a new class of two-photon pumped lasing dyes. J Mater Chem 13:2499–2504
25. Yang YQ, Li CH, Li W, Yi ZJ (2010) Hydrothermal synthesis, crystal structure and luminescent property of Tb(III) complex by *m*-chlorobenzoic acid ligand. Chin J Inorg Chem 26:546–550
26. Li YQ, Ju YL, Zhang YB, Wang CY, Zhang TT, Li X (2007) Synthesis, crystal and characterization of two terbium complexes with bromobenzoic acid. Chin J Inorg Chem 23:969–974
27. Dong YB, Smith MD, Loye HC (2000) Novel M(II)-Hg(II) coordination polymers generated from metal-containing building blocks $M(2\text{-pyrazinecarboxylate})_2\ (H_2O)_2$ (M=Cu, Ni, Co) and $HgCl_2$. Solid State Sci 2:861–870
28. Abbotto A, Beverina L, Bozio R, Facchetti A, Ferrante C, Pagani GA, Pedron D, Signorini R (2003) Novel heteroaromatic-based multi-branched dyes with enhanced two-photon absorption activity. Chem Commun 2144–2145
29. Lee HJ, Sohn J, Hwang J, Park SY, Choi H, Cha M (2004) Triphenylamine-cored bifunctional organic molecules for two-photon absorption and photorefraction. Chem Mater 16:456–465
30. Chen HH, Liu ZQ, Cao DX, Deng YL, Sun YH, Li FY (2013) Synthesis and photophysical properties of two novel branched pyridinium inner salt dyes. Dyes Pigments 96:563–568
31. Aranda AI, Achelle S, Hammerer F, Mahuteau-Betzer F, Teulade-Fichou M (2012) Vinyl-diazine triphenylamines and their N-methylated derivatives: synthesis, photophysical properties and application for staining DNA. Dyes Pigments 95:400–407
32. Ozturk G, Karakas D, Karadag F, Ozturk G, Yorgun C (2012) Synthesis and characterization of new Y-shaped fluorophores with an imidazole core. J Fluoresc 22:1159–1164
33. Sarkar N, Das K, Nath DN, Bhattacharyya K (1994) Twisted charge transfer processes of nile red in homogeneous solutions and in faujasite zeolite. Langmiur 10:326–329